

1 **Control flow in active inference systems**

2 **Part I:**

3 **Classical and quantum formulations of active**

4 **inference**

5 Chris Fields<sup>a,\*</sup>, Filippo Fabrocini<sup>b,c</sup>, Karl Friston<sup>d,e</sup>, James F. Glazebrook<sup>f,g</sup>,  
Hananel Hazan<sup>a</sup>, Michael Levin<sup>a,h</sup> and Antonino Marcianò<sup>i,j,k</sup>

<sup>a</sup> *Allen Discovery Center at Tufts University, Medford, MA 02155 USA*

<sup>b</sup> *College of Design and Innovation, Tongji University, 281 Fuxin Rd,  
200092 Shanghai, CHINA*

<sup>c</sup> *Institute for Computing Applications “Mario Picone”,  
Italy National Research Council, Via dei Taurini, 19, 00185 Rome, ITALY*

<sup>d</sup> *Wellcome Centre for Human Neuroimaging, University College London,  
London, WC1N 3AR, UK*

<sup>e</sup> *VERSES Research Lab, Los Angeles, CA, 90016 USA*

<sup>f</sup> *Department of Mathematics and Computer Science,  
Eastern Illinois University, Charleston, IL 61920 USA*

<sup>g</sup> *Adjunct Faculty, Department of Mathematics,  
University of Illinois at Urbana-Champaign, Urbana, IL 61801 USA*

<sup>h</sup> *Wyss Institute for Biologically Inspired Engineering at Harvard University,  
Boston, MA 02115, USA*

<sup>i</sup> *Center for Field Theory and Particle Physics & Department of Physics  
Fudan University, Shanghai, CHINA*

<sup>j</sup> *Laboratori Nazionali di Frascati INFN, Frascati (Rome), ITALY*

<sup>k</sup> *INFN sezione Roma “Tor Vergata”, I-00133 Rome, ITALY*

## 7 **Abstract**

8 Living systems face both environmental complexity and limited access to free-energy re-  
9 sources. Survival under these conditions requires a control system that can activate, or  
10 deploy, available perception and action resources in a context specific way. In this Part I,  
11 we introduce the free-energy principle (FEP) and the idea of active inference as Bayesian  
12 prediction-error minimization, and show how the control problem arises in active inference  
13 systems. We then review classical and quantum formulations of the FEP, with the former  
14 being the classical limit of the latter. In the accompanying Part II, we show that when  
15 systems are described as executing active inference driven by the FEP, their control flow  
16 systems can always be represented as tensor networks (TNs). We show how TNs as control  
17 systems can be implemented within the general framework of quantum topological neural  
18 networks, and discuss the implications of these results for modeling biological systems at  
19 multiple scales.

20

## 21 **Keywords**

22 Bayesian mechanics; Dynamic attractor; Free-energy principle; Quantum reference frame;  
23 Scale-free model; Topological quantum field theory

24

## 25 **1 Introduction**

26 Living things offer remarkable examples of complex, multi-level control policies that guide  
27 adaptive function at several scales. At the same time, they are made of components which

---

\*Corresponding author at: Allen Discovery Center at Tufts University, Medford, MA 02155 USA; *E-mail address:* fieldsres@gmail.com

28 are usually thought of as physical objects obeying simple rules; how can these two per-  
29 spectives be unified in a rigorous manner? The framework of *active inference* answers this  
30 question, by providing a completely general, scale-free formal framework for describing in-  
31 teractions between physical systems in cognitive terms. It is based on the Free Energy  
32 Principle (FEP), first introduced in neuroscience [1, 2, 3, 4, 5] before being extended to  
33 living systems in general [6, 7, 8, 9] and then to all self-organizing systems [10, 11, 12, 13].  
34 The FEP states that any system that interacts with its environment weakly enough to  
35 maintain its identifiability over time 1) has a Markov blanket (MB) that separates its inter-  
36 nal states from the states of its environment [14, 15, 16, 17, 18] and 2) behaves over time in  
37 a way that asymptotically minimizes a variational free energy (VFE) measured at its MB.  
38 Equivalently, the FEP states that any system with a non-equilibrium steady-state (NESS)  
39 solution to its density dynamics (and hence an MB) will act so as to maintain its state in  
40 the vicinity of its NESS. Any system compliant with the FEP can be described as engaging,  
41 at all times, in active inference: a cyclic process in which the system observes its environ-  
42 ment, updates its probabilistic “Bayesian beliefs” (i.e., posterior or conditional probability  
43 densities) over future behaviors, and acts on its environment so as to test its predictions  
44 and gain additional information. The internal dynamics of such a system can be described  
45 as inverting a generative model (GM) of its environment that furnishes predictions of the  
46 consequences of its actions on its MB.

47 As a fully-general principle, the FEP applies to all physical systems, not just to behav-  
48 iorally interesting, plausibly cognitive systems, such as organisms or autonomous robots  
49 [10]. Intuitively, behavior is interesting – to external observers and, we can assume, to  
50 the behaving system itself – when it is complex, situation-appropriate, and robust in the  
51 face of changing environmental conditions. Friston et al. [13] characterize interesting sys-  
52 tems as “strange particles”, whose internal (i.e., cognitive) states are influenced by their  
53 actions only via perceived environmental responses; such systems have to “ask questions”

54 of their environments in order to get answers [19]. Such systems, even bacteria and other  
55 basal organisms [20, 21, 22, 23], have multiple ways of observing and acting upon their  
56 environments and deploy these resources in context-sensitive ways. In operations-research  
57 language, they exhibit situational awareness, i.e., awareness of the context of actions [24],  
58 and deploy attention systems to manage the informational, thermodynamic, and metabolic  
59 costs of maintaining such awareness [12, 22]. Situational awareness is dependent on both  
60 short- and long-term memory, or more technically, on the period of time over which precise  
61 [Bayesian] beliefs exist, sometimes referred to as the temporal depth or horizon of the GM  
62 [20, 21]. Upper limits can, therefore, be placed on behavioral complexity by examining  
63 the capacity and control of memory systems from the cellular scale [25] upwards. Liv-  
64 ing systems from microbial mats to human societies employ stigmergic memories [22] and  
65 hence have “extended minds” [26] in the sense of the literature on embodied, embedded,  
66 enactive, extended, and affective (4EA) cognition [27, 28]. Such memories must be both  
67 readable and writable; hence any system using them must have dedicated, memory-specific  
68 perception–action capabilities.

69 Any system with multiple perception–action (or stimulus–response) capabilities requires a  
70 control system that enables context-guided perception and action and precluding the con-  
71 tinuous, simultaneous deployment of all available perception–action capabilities. Such self  
72 organization entails the selection of a particular course of action – i.e., policy – from all  
73 plausible policies entertained by the system’s GM. In the active inference framework, the  
74 system’s internal states – hence its GM – can be read as encoding posterior probability  
75 densities (i.e., Bayesian beliefs) over the causes of its sensory states, including, crucially, its  
76 own actions. This leads to the notion of planning and control as inference [29, 30, 31], with  
77 the ensuing selection of an action given by the most likely policy. In bacteria such as *E.*  
78 *coli*, for example, mutual inhibition between gene regulatory networks (GRNs) for different  
79 metabolic operons permit the expression of specific carbon-source (e.g., sugar) metabolism

80 pathways only when the target carbon source is detected in the environment [32]. The con-  
81 trol of foraging behavior via chemotaxis employs a similar, in this case bistable, mechanism  
82 [33]. Such mechanisms are active in multicellular morphogenesis, for example, in the head-  
83 versus-tail morphology decision in planaria [34]. In the human brain, mutual inhibition  
84 between competing visual processing streams is evident in binocular rivalry (switching be-  
85 tween distinct scenes presented to left and right eyes) or in the changing interpretations of  
86 ambiguous figures such as the Necker cube [35, 36]; similar competitive effects are observed  
87 in other sensory pathways [37]. It also characterizes the competitive interaction between the  
88 dorsal and ventral attention systems, which implement top-down and bottom-up targeting  
89 of sensory resources, respectively [38]. It is invoked at a still larger scale in global workspace  
90 models of conscious processing, in which incoming information streams must compete, with  
91 each inhibiting the others, for “access to consciousness” [39, 40]. Mutual inhibition cre-  
92 ates an energetic barrier that the control system that implements switching must expend  
93 free-energy resources to overcome; the controller must not only turn “on” the preferred  
94 system, but also turn “off” the inhibition. The required free energy expenditure in turn  
95 induces hysteresis and hence the non-linear, winner-takes-all “switch” behavior in the time  
96 regime. Such barriers and their temporal consequences persist in more complex control  
97 systems whenever two perception–action capabilities are either functionally incompatible  
98 or too expensive to deploy simultaneously.

99 Switching between perception–action capabilities can be regarded, from a theoretical, FEP  
100 perspective, as selecting a plausible policy, or plan, supported by the GM. Technically, the  
101 probability distribution over policies or plans can be computed from a free energy functional  
102 expected under the posterior predictive density over possible outcomes, as described in §2.1  
103 below. The control system that implements the switching process can be considered to  
104 employ the GM to predict, or assign a probability distribution to, each perception-action  
105 capability (i.e., policy) as a function of context [41, 42]. We can consider the GM to

106 generate probabilistic “beliefs” about the consequences of actions, where here a “belief” is  
107 just a mathematically-described structure, e.g., a classical conditional probability density  
108 or a quantum state with an assigned amplitude. “Planning” or “control” can, therefore,  
109 always be cast as inference – again in the basal sense of computation – implemented by  
110 variational message passing or “belief propagation” on a (normal style) factor graph: a  
111 graph with nodes corresponding to the factors of a probability distribution and undirected  
112 edges corresponding to message-passing channels. Factor graphs can be combined with  
113 message passing schemes, with the messages generally corresponding to sufficient statistics  
114 of the factors in question, to provide an efficient computation of functions such as marginal  
115 densities [43, 44]. Hence one can formalize control – under the FEP – in terms of control as  
116 inference, which implies that there is a description of control in terms of message passing  
117 on a factor graph. When the GM is over discrete states, this implies a description of control  
118 in terms of tensor operators.

119 Nearly all simulations of planning – under discrete state space GMs – use the factor-  
120 graph formalism. Crucially, the structure of the factor graph embodies the structure of the  
121 GM and, effectively, the way that any system represents the (apparent causes of) data on  
122 its MB; i.e., the way it “carves nature at its joints,” into states, objects and categorical  
123 features. Under the (classical) FEP, the factors that constitute the nodes of the factor  
124 graph correspond to the state-space factorization in a mean field approximation, as used  
125 by physicists, or by statisticians to implement variational Bayesian (a.k.a., approximate  
126 Bayesian) inference [45]. See [46] for technical details, [47] for an application to the brain,  
127 and Supplementary Information, Table 1 for a list of selected applications.

128 We show in Parts I and II of this paper that control flow in such systems can always be  
129 formally described as a tensor network, a factorization of some overall tensor (i.e., high-  
130 dimensional matrix) operator into multiple component tensor operators that are pairwise  
131 contracted on shared degrees of freedom [48]. In particular, we show that the factorization

132 conditions that allow the construction of a TN are exactly the same as those that allow  
133 the identification of distinct, mutually conditionally independent (in quantum terms, de-  
134 coherent), sets of data on the MB, and hence allow the identification of distinct “objects”  
135 or “features” in the environment. This equivalence allows the topological structures of  
136 TNs – many of which have been well-characterized in applications of the TN formalism  
137 to other domains [48] – to be employed as a classification of control structures in active  
138 inference systems; including cells, organisms, and multi-organism communities. It allows,  
139 in particular, a principled approach to the question of whether, and to what extent, a  
140 cognitive system can impose a decompositional or mereological (i.e., part-whole) structure  
141 on its environment. Such structures naturally invoke a notion of locality, and hence of  
142 geometry. The geometry of spacetime itself has been described as a particular TN – a  
143 multiscale entanglement renormalization ansatz (MERA) [49, 50, 51] – suggesting a deep  
144 link between control flow in systems capable of observing spacetime (i.e., capable of im-  
145 plementing internal representations of spacetime) and the deep structure of spacetime as a  
146 physical construct.

147 We begin in this Part I, §2 by analyzing the control-flow problem in three different rep-  
148 resentations of active inference. First, we employ the classical, statistical formulation of  
149 the FEP [10, 11] in §2.1 to describe control flow as implementing discrete, probabilistic  
150 transitions between dynamical attractors on a manifold of computational states. We then  
151 reformulate the physical interaction in quantum information-theoretic terms in §2.2; in this  
152 formulation [12], components of the GM can be considered to be distinct quantum refer-  
153 ence frames (QRFs) [52, 53] and represented by hierarchical networks of Barwise-Seligman  
154 classifiers [54] as developed in [55, 56, 57, 58]. Control flow then implements discrete tran-  
155 sitions between QRFs. The third step, in §2.3, employs the mapping between hierarchies  
156 of classifiers and topological quantum field theories (TQFTs) developed in [59]. Here, con-  
157 trol flow is implemented by a TQFT, with transition amplitudes given by a path integral.



158 The second and third of these representations provide formal characterizations of intrinsic  
159 (or “quantum”) context effects that are consistent with both the sheaf-theoretic treatment  
160 of contextuality in [60, 61] and the Contextuality by Default (CbD) approach of [62, 63];  
161 see also the discussion in [57] and [59, §7.2]. The underlying theme is that contextuality  
162 arises due to the non-existence of any globally definable (maximally connected) conditional  
163 probability distribution across all possible observations (see e.g., [64] for a review from a  
164 more general physics perspective). Extending our earlier analysis [57], we discuss reasons  
165 to expect that active inference systems will generically exhibit such context effects.

166 In Part II, we develop a fully-general tensor representation of control flow, and prove that  
167 this tensor can be factored into a TN if, and only if, the separability (or conditional sta-  
168 tistical independence) conditions needed to identify distinct features of, or objects in, the  
169 environment are met. We show how TN architecture allows classification of control flows,  
170 and give two illustrative examples. We then discuss several established relationships be-  
171 tween TNs and artificial neural network (ANN) architectures, and show how these generalize  
172 to topological quantum neural networks [59, 65], of which standard deep-learning (DL) ar-  
173 chitectures are a classical limit [66]. Having developed these formal results, we turn to  
174 implications of these results for biology, and discuss how TN architectures correlate with  
175 the observational capabilities of the system being modeled, particularly as regards abilities  
176 to detect spatial locality and mereology. We consider how to classify known control path-  
177 ways in terms of TN architecture and how to employ the TN representation of control flow  
178 in experimental design. We conclude by looking forward to how these FEP-based tools can  
179 further integrate the physical and life sciences.

## 2 Formal description of the control problem

### 2.1 The attractor picture

Let  $U$  be a random dynamical system that can be decomposed into subsystems with states  $\mu(t)$ ,  $b(t)$ , and  $\eta(t)$  such that the dependence of the  $\mu(t)$  on the  $\eta(t)$ , and vice-versa, is only via the  $b(t)$ . In this case, the  $b(t)$  form an MB separating the  $\mu(t)$  from the  $\eta(t)$ . We will refer to the  $\mu(t)$  as “internal” states, to the  $\eta(t)$  as “environment” states, and to the combined  $\pi(t) = (b(t), \mu(t))$  as “particular” (or “particle”) states [10]. The FEP is a variational or least-action principle stating that any system – that interacts sufficiently weakly with its environment – can be considered to be enclosed by an MB, i.e. any “particle” with states  $\pi(t) = (b(t), \mu(t))$ , will evolve in a way that tends to minimize a variational free energy (VFE)  $F(\pi)$  that is an upper bound on (Bayesian) surprisal. This free energy is effectively the divergence between the variational density encoded by internal states and the density over external states conditioned on the MB states. It can be written [10, Eq. 2.3],

$$\begin{aligned}
 F(\pi) &= \underbrace{\mathbb{E}_{q(\eta)}[\ln q_\mu(\eta) - \ln p(\eta, b)]}_{\text{Variational free energy}} \\
 &= \underbrace{\mathbb{E}_q[-\ln p(b|\eta) - \ln p(\eta)]}_{\text{Energy constraint (likelihood \& prior)}} - \underbrace{\mathbb{E}_q[-\ln q_\mu(\eta)]}_{\text{Entropy}} \\
 &= \underbrace{D_{KL}[q_\mu(\eta)|p(\eta)]}_{\text{Complexity}} - \underbrace{\mathbb{E}_q[\ln p(b|\eta)]}_{\text{Accuracy}} \\
 &= \underbrace{D_{KL}[q_\mu(\eta)||p(\eta|b)]}_{\text{Divergence}} - \underbrace{\ln p(b)}_{\text{Log evidence}} \geq -\ln p(b)
 \end{aligned} \tag{1}$$

The VFE functional  $F(\pi)$  is an upper bound on surprisal (a.k.a. self-information)  $\mathfrak{I}(\pi) = -\ln p(\pi) > -\ln p(b)$  because the Kullback-Leibler divergence term ( $D_{KL}$ ) is always non-negative. This KL divergence is between the density over external states  $\eta$ , given the MB state  $b$ , and a variational density  $q_\mu(\eta)$  over external states parameterized by the internal

197 state  $\mu$ . If we view the internal state  $\mu$  as encoding a posterior over the external state  $\eta$ ,  
198 minimizing VFE is, effectively, minimizing a prediction error, under a GM encoded by the  
199 NESS density. In this treatment, the NESS density becomes a probabilistic specification  
200 of the relationship between external or environmental states and particular (i.e., “self”)  
201 states. We can interpret the internal and active MB states in terms of active inference,  
202 i.e., a Bayesian mechanics [11], in which their expected flow can be read as perception  
203 and action, respectively. Here “active” states are a subset of the MB states that are not  
204 influenced by environmental states and – for the kinds of particles considered here – do  
205 not influence internal states. In other words, active inference is a process of Bayesian  
206 belief updating that incorporates active exploration of the environment. It is one way  
207 of interpreting a generalized synchrony between two random dynamical systems that are  
208 coupled via an MB.

209 If the “particle”  $\pi$  is a biological cell, it is natural to consider the MB  $b$  to be implemented  
210 by the cell membrane and the “internal” states  $\mu$  to be the internal macromolecular or  
211 biochemical states of the cell; indeed, it is this association that motivated the application of  
212 the FEP to cellular life [5]. In this case, the NESS corresponds to the state, or neighborhood  
213 of states, that maintain homeostasis (or more broadly, allostasis [67, 68, 69]) and hence  
214 maintain the structural and functional integrity of  $\pi$  as a living cell. This activity of self-  
215 maintenance has been termed “self-evidencing” [70]; systems compliant with the FEP can  
216 be considered to be continually generating evidence of – or for – their continued existence  
217 [10].

218 In the terminology of [13] cells are “strange particles” – their signal transduction pathways  
219 monitor (components of) the states of their environments, but do not directly monitor their  
220 actions on their environments (i.e., their own active states). The consequences of any action  
221 can only, therefore, be deduced from the response of the environment. In this situation,  
222 causation is always uncertain: whether an action by the environment on the cell – what

223 the cell detects as an environmental state change – is a causal consequence of an action the  
224 cell has taken in the past cannot be determined by the data available to the cell. Every  
225 action, therefore, increases VFE, while every observation (potentially) decreases it. The  
226 (apparent) task of the cell’s GM is to minimize the increases, on average, while maximizing  
227 the decreases.

228 The Bayesian mechanics afforded by the FEP implies a (classical) thermodynamics; indeed,  
229 the FEP can be read as a constrained maximum entropy or caliber principle [71, 72]. This  
230 follows from the fact that inference, i.e., self evidencing, entails belief updating and belief  
231 updating incurs a thermodynamic cost via the Jarzynski equality [73, 74, 75]. This cost  
232 provides a lower bound on the thermodynamic free energy required for metabolic mainte-  
233 nance. For example, a cell’s actions on its environment – e.g., chemotactic locomotion – are  
234 largely driven by the need to acquire thermodynamic free energy. The cell’s GM cannot,  
235 therefore, minimize VFE by minimizing action [76]; instead, it must successfully predict  
236 which actions will replenish its free-energy supply. As actions are energetically expensive,  
237 this requires trading off short-term costs against long-term goals. As shown in [41], selective  
238 pressures operating on different timescales favor the development of metaprocessors that  
239 control lower-level actions in a context-dependent way; these are often implemented via a  
240 hierarchical GM [77]. Such meta-level control provides probabilistic models of risk-sensitive  
241 actions in context.

242 While such systems may be described as regulating free-energy seeking actions, they also  
243 regulate information-seeking actions, i.e., curiosity-driven exploration [78, 79, 80]. This  
244 follows because VFE provides an upper bound on complexity minus accuracy [81]. The  
245 expected free energy (EFE), conditioned upon any action, can therefore be scored in terms  
246 of expected complexity and expected inaccuracy. Expected complexity is “risk” and cor-  
247 responds to the degree of belief updating that incurs a thermodynamic cost; leading to  
248 risk-sensitive control (e.g., phototropism). Expected inaccuracy corresponds to “ambigu-

ity” leading to epistemic behaviors (e.g., searching for lost keys under a streetlamp) [42].

When context-dependent control is considered, the neighborhood of the NESS resolves into a network of local minima corresponding to fixed perception-action loops separated by energetic barriers that the control system must overcome to switch between loops. For example, in a cell, this energetic barrier comprises the energy required to activate one pathway while de-activating another, which may include the energetic costs of phosphorylation, other chemical modifications, additional gene expression, etc. Different pairs of pathways can be expected to be separated by energetic barriers of different heights, generating a topographically-complex free energy landscape that coarse-grains, in a long-time average, to the neighborhood of the NESS, i.e., to the maintenance of allostasis [68, 69, 82].

As noted earlier, we can think of controllable perception-action loops as nodes on a factor graph, with the edges corresponding to pathways for control flow, and the transition probabilities labeling the edges as inversely proportional to the energetic barrier between loops. This allows representing the GM for meta-level (i.e., hierarchical) control as a message-passing system as described in [47]. The presence of very high energetic barriers can render such a GM effectively one-way, as seen in the context-dependent switches between signal transduction pathways and GRNs that characterize cellular differentiation during morphogenesis. Biological examples of these include modifications of bioelectric pattern memories in planaria, which can create alternative-species head shapes that eventually remodel back to normal [83], or produce 2-headed worms which are permanent, and regenerate as 2-headed in perpetuity [84].

## 2.2 The QRF picture

Cellular information processing has traditionally been treated as completely classical, i.e., as implemented by causal networks of macromolecules, each of which undergoes classical

273 state transitions via local dynamical processes that are conditionally independent of the  
 274 states of other parts of the network. While the “quantum” nature of proteins and other  
 275 macromolecules is broadly acknowledged, the scale at which quantum effects are important  
 276 remains controversial, with straightforward single-molecule decoherence models predicting  
 277 decoherence times of attoseconds ( $10^{-18}$  s) or less [85, 86]: several orders of magnitude  
 278 below the timescales of processes involved in molecular information processing [87]. While  
 279 functional roles for quantum coherence in intramolecular information processing have been  
 280 demonstrated, intermolecular coherence remains experimentally elusive [88, 89, 90, 91].

281 The free-energy budgets of both prokaryotic and eukaryotic cells are, however, orders of  
 282 magnitude smaller than would be required to support fully-classical information processing  
 283 at the molecular scale, suggesting that cells employ quantum coherence as a computational  
 284 resource [92]. Indirect evidence of longer-range, tissue-scale coherence in brains has also  
 285 been reported [93]. Reformulating the FEP in quantum information-theoretic terms enables  
 286 it to describe situations in which long-range coherence, and hence quantum computation,  
 287 cannot be neglected.

288 Following the development in [12], we consider a bipartite decomposition  $U = AB$  of a  
 289 finite, isolated system  $U$  for which the interaction Hamiltonian  $H_{AB} = H_U - (H_A + H_B)$  is  
 290 sufficiently weak over the time period of interest that the joint state  $|U\rangle$  is separable (i.e.,  
 291 factors) as  $|U\rangle = |A\rangle|B\rangle$ . In this case, we can choose orthogonal basis vectors  $|i^k\rangle$  so that:

$$H_{AB} = \beta_k K_B T_k \sum_i^N \alpha_i^k M_i^k, \quad (2)$$

292 where  $K_B$  denotes Boltzmann’s constant,  $T$  is the absolute temperature of the environment,  
 293  $k = A$  or  $B$ , the  $M_i^k$  are  $N$  mutually-orthogonal Hermitian operators with eigenvalues in  
 294  $\{-1, 1\}$ , the  $\alpha_i^k \in [0, 1]$  are such that  $\sum_i^N \alpha_i^k = 1$ , and  $\beta_k \geq \ln 2$  is an inverse measure of  $k$ ’s  
 295 thermodynamic efficiency that depends on the internal dynamics  $H_k$ ; see [56, 58, 94, 95] for

296 further motivation and details of this construction and [96] for a pedagogical review. This  
 297 description is purely topological, attributing no geometry to either  $U$  or  $\mathcal{B}$ ; hence it allows  
 298 the “embedding space” of perceived “objects” to be an observer-dependent construct. It  
 299 has several relevant consequences:

- 300 • We can regard  $A$  and  $B$  as separated, and determined by independent measures. They  
 301 are separated by – and interact via – a holographic screen  $\mathcal{B}$  that can be represented,  
 302 without loss of generality, by an array of  $N$  non-interacting qubits, where  $N$  is the  
 303 dimension of  $H_{AB}$  [94, 95].
- 304 •  $A$  and  $B$  can be regarded as exchanging finite  $N$ -bit strings, each of which encodes  
 305 one eigenvalue of  $H_{AB}$  [94].
- 306 •  $A$  and  $B$  have free choice of basis for  $H_{AB}$ , corresponding to free choice of local frames  
 307 at  $\mathcal{B}$ , e.g., free choice, for each qubit  $q_i$  on  $\mathcal{B}$ , of the local  $z$  axis and hence the  $z$ -spin  
 308 operator  $s_z$  that acts on  $q_i$  [96].
- 309 • Choice of basis corresponds to choosing the zero-point of total energy by each of  $A$   
 310 and  $B$ . The systems  $A$  and  $B$  are, therefore, in general at informational, but not at  
 311 thermal equilibrium [12].
- 312 • As  $A$  and  $B$  must obtain from  $B$  or  $A$ , respectively, whatever thermodynamic free  
 313 energy is required, by Landauer’s principle [73, 99, 100], to fund the encoding of  
 314 classical bits on  $\mathcal{B}$  (as well as any other irreversible classical computation),  $A$  and  $B$   
 315 must each devote some sector  $F$  of  $\mathcal{B}$  to free-energy acquisition. The bits in  $F$  are  
 316 “burned as fuel” and so do not contribute input data to computations. Waste-heat  
 317 dissipation by one system is free energy acquisition by the other. The free-energy  
 318 sectors  $F_A$  and  $F_B$  of  $A$  and  $B$  need not align as subsets of qubits on  $\mathcal{B}$ ; that is,

319 qubits that  $A$  regards as free-energy sources may be regarded by  $B$  as informative  
 320 outputs and vice-versa [56, 58].

- 321 • The actions of the internal dynamics  $H_A$  and  $H_B$  on  $\mathcal{B}$  can be represented by  $A$ -  
 322 and  $B$ -specific sets of QRFs, each of which both “measures” and “prepares” qubits  
 323 on  $\mathcal{B}$ . Each QRF acts on the qubits in some specific sector of  $\mathcal{B}$ , breaking the  
 324 permutation symmetry of Eq. (2) [56, 58, 59]. Only QRFs acting on sectors other  
 325 than  $F$  implement informative computations; we will therefore restrict attention to  
 326 these QRFs.
- 327 • Each “computational” QRF can, without loss of generality, be represented by a cone-  
 328 cocone diagram (CCCD) comprising Barwise-Seligman classifiers and infomorphisms  
 329 between them [54, 55]. The apex of each such CCCD is, by definition, both the  
 330 category-theoretic limit and colimit of the “input/output” classifiers that correspond,  
 331 formally, to the operators  $M_i^k$  in Eq. (2) [56, 58, 59].

332 Typically, a CCCD is structured as a distributed information flow in the form:

$$\begin{array}{ccccccc}
 \mathcal{A}_1 & \xleftrightarrow{g_{21}} & \mathcal{A}_2 & \xleftrightarrow{g_{32}} & \dots & \mathcal{A}_k & \\
 & \xleftarrow{g_{12}} & & \xleftarrow{g_{23}} & & & \\
 & & \mathbf{C}' & & & & \\
 & \xleftarrow{h_1} & \uparrow h_2 & \xrightarrow{h_k} & & & \\
 & & \mathbf{C}' & & & & \\
 & \xrightarrow{f_1} & \downarrow f_2 & \xleftarrow{f_k} & & & \\
 \mathcal{A}_1 & \xleftrightarrow{g_{21}} & \mathcal{A}_2 & \xleftrightarrow{g_{32}} & \dots & \mathcal{A}_k & \\
 & \xleftarrow{g_{12}} & & \xleftarrow{g_{23}} & & & 
 \end{array} \tag{3}$$

333 incorporating sets of classifiers  $\{\mathcal{A}_\alpha\}$  and (logic) infomorphisms  $\{f_i, g_{jk}\}$  [54, Ch 12] over  
 334 suitable index ranges. As a memory-write system, Diagram (3) depicts a generic blueprint  
 335 for a bow-tie or variational autoencoder (VAE) network amenable to describing a hierar-  
 336 chical Bayesian network with belief-updating as discussed in e.g. [12, 57, 59]. Crucially, it  
 337 is the non-commutativity of CCCDs of this form that specifies intrinsic or quantum con-



338 textuality, as occurs, for instance, when the colimit core  $\mathbf{C}'$  is undefinable [57, §7, §8] [59,  
 339 §7.2]. Consequences of such contextuality are discussed via examples in Part II.

340 The holographic screen  $\mathcal{B}$  functions as an MB separating  $A$  from  $B$ . It can be regarded  
 341 as having an  $N$ -dimensional,  $N$ -qubit Hilbert space  $\mathcal{H}_{q_i} = \prod_i q_i$ . While  $\mathcal{H}_{q_i}$  is strictly  
 342 ancillary to  $\mathcal{H}_U = \mathcal{H}_A \otimes \mathcal{H}_B$ , the classical situation can be recovered in the limit in which  
 343 the entanglement entropies  $\mathcal{S}(|A\rangle), \mathcal{S}(|B\rangle) \rightarrow 0$  by considering the products  $\mathcal{H}_A \otimes \mathcal{H}_{q_i}$  and  
 344  $\mathcal{H}_B \otimes \mathcal{H}_{q_i}$  to be “particle” state spaces for  $A$  and  $B$ , respectively. In this classical limit, the  
 345 states of  $\mathcal{H}_{q_i}$  become the blanket states of an MB that functions as a classical information  
 346 channel [94, 95, 96]. In quantum holographic coding, for example,  $\mathcal{B}$  is often represented  
 347 by a polygonal tessellation of the hyperbolic disc, with qubits represented by polygonal  
 348 centroids. A specific TN model of a pentagon code is developed in [97]; see in particular  
 349 their Fig. 4. The geometric description of  $\mathcal{B}$  as implementing holographic coding, and its  
 350 classical limit as an MB structured as a direct acyclic graph (DAG), is further explored in  
 351 the setting of TQNNs in [98].

352 In this quantum-theoretic picture, “systems” or “objects” observed and manipulated by  
 353  $A$  or  $B$  correspond to sectors on  $\mathcal{B}$  that are the domains of particular QRFs deployed  
 354 by  $A$  or  $B$ , respectively [58, 12, 59]. To simplify notation, we use the same symbol, e.g.,  
 355 ‘ $Q$ ’ to denote both a QRF  $Q$  and the sector  $\text{dom}(Q)$  on  $\mathcal{B}$ . Any identifiable system  $X$   
 356 factors into a “reference” component  $R$  that maintains a time-invariant state  $|R\rangle$  or more  
 357 generally, state density  $\rho_R$ , that allows re-identification and hence sequential measurements  
 358 over extended time, and a “pointer” component  $P$  with a time-varying state  $|P\rangle$  or density  
 359  $\rho_P$ . It is this pointer component, named for the pointer of an analog instrument, which  
 360 is the “state of interest” for measurements. The QRFs  $R$  and  $P$  clearly must commute,  
 361 and the sectors  $R$  and  $P$  clearly must be mutually decoherent [58, 12, 59]. All “system”  
 362 sectors must be components of some overall sector  $E$  that corresponds to the “observable  
 363 environment.” The recording of measurement outcomes to a classical memory and the

364 reading of previously-recorded outcomes from memory can similarly be represented by a  
 365 QRF  $Y$ . As  $\text{dom}(Y)$  is a sector on  $\mathcal{B}$ , recorded memories of  $A$  are exposed to and hence  
 366 subject to modification by  $B$  and vice-versa. Both the observable environment  $E$  and the  
 367 memory sector  $Y$  must be disjoint from, and decoherent with, the free-energy sector  $F$ .  
 368 As actions on  $\mathcal{B}$  encode classical data, they have an associated free energy cost of at  
 369 least  $\ln 2 K_B T$  per bit [73, 99, 100] that must originate from the source at  $F$ . Time-  
 370 energy complementarity associates a minimum time of  $h/[\ln 2(K_B T)]$ , with  $h$  being Planck's  
 371 constant, to this energy expenditure. We can, therefore, associate actions on  $\mathcal{B}$ , including  
 372 memory writes, with “ticks” of an internal time QRF, which we denote  $t_A$  and  $t_B$  for  $A$   
 373 and  $B$ , respectively. Assuming all observational outcomes are written to memory, we can  
 374 represent the situation as in Fig. 1. The time QRF is effectively an outgoing bit counter  
 375 that can be represented by a groupoid operator  $\mathcal{G}_{ij} : t_i \rightarrow t_j$  [56]. As outgoing bits are  
 376 oriented in opposite directions with respect to  $\mathcal{B}$  for  $A$  and  $B$ , the time “arrows”  $t_A$  and  
 377  $t_B$  point in opposite directions. Hence  $A$  and  $B$  can both be regarded as “interacting with  
 378 their own futures” as discussed in [96].

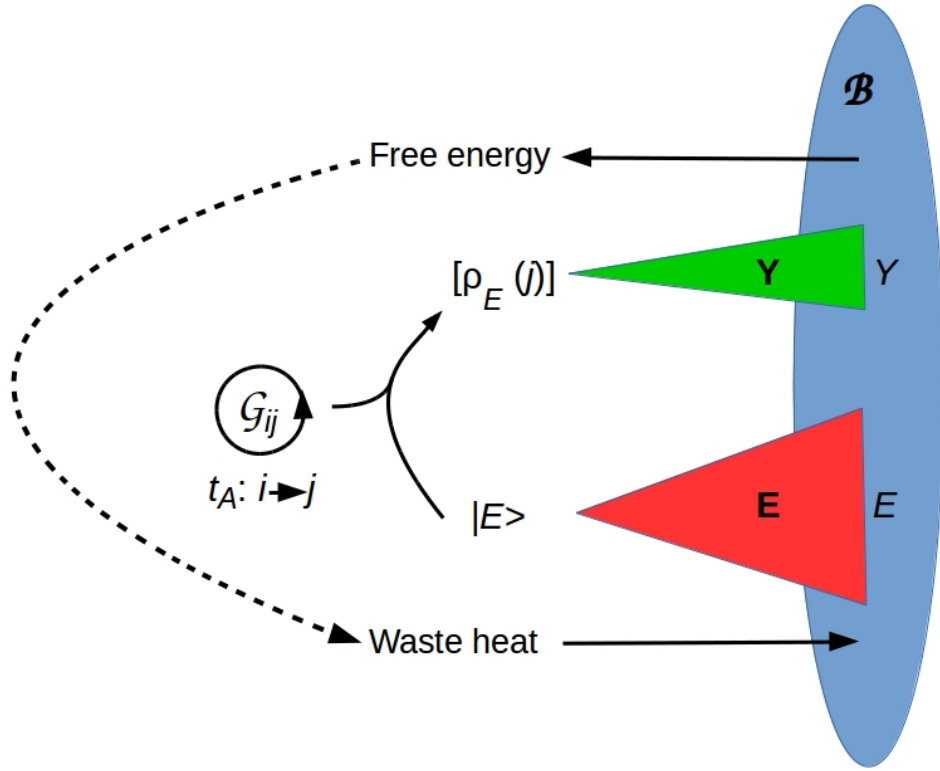
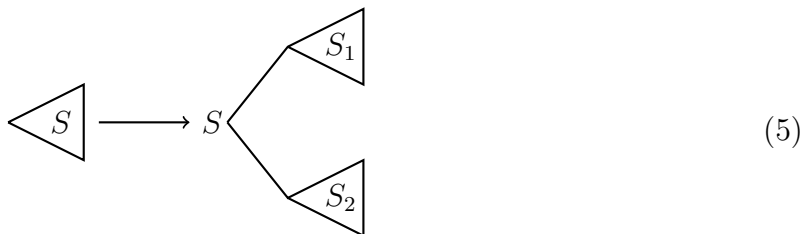


Figure 1: Cartoon illustration of QRFs required to observe and write a readable memory of an environmental state  $|E\rangle$ . The QRFs  $\mathbf{E}$  and  $\mathbf{Y}$  read the state from  $E$  and write it to the memory  $Y$  respectively. Any identified system  $S$  must be part of  $E$ . The clock  $\mathcal{G}_{ij}$  is a time QRF that defines the time coordinate  $t_A$ . The dashed arrow indicates the observer's thermodynamic process that converts free energy obtained from the unobserved sector  $F$  of  $\mathcal{B}$  to waste heat exhausted through  $F$ . Adapted from [58], CC-BY license.

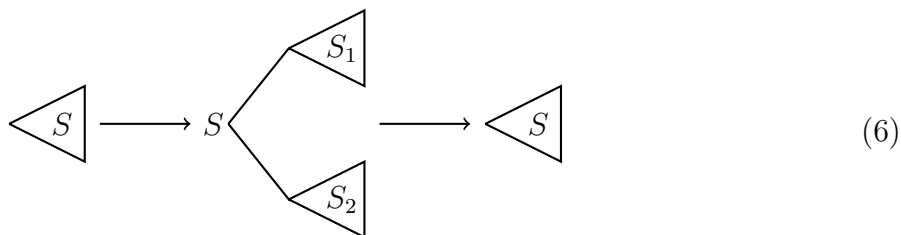
379 Measurements of a system  $X$  can be considered sequential if: 1) they are separated in  
 380 time according to the internal time QRF, and 2) their outcomes are recorded to memory  
 381 to enable comparability across time. We show in [59] that sequential measurements can  
 382 always be represented by one of two schemata. Using the compact notation:

$$\begin{array}{c} \triangle \\ S \end{array} \tag{4}$$

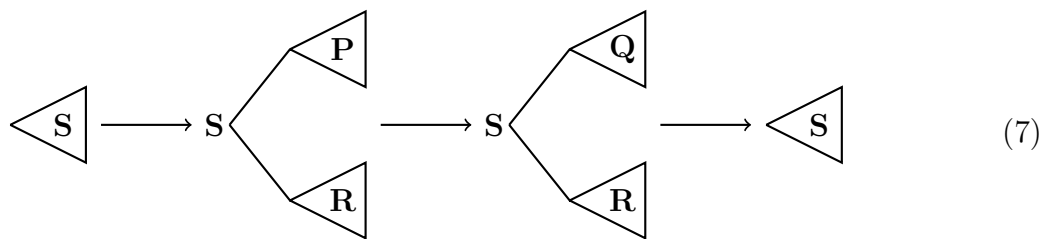
383 to represent a QRF  $S$ , we can represent measurements of a physical situation in which one  
 384 system divides into two, possibly entangled, systems with a diagram of the form:



385 Parametric down-conversion of a photon exemplifies this kind of process. The reverse  
 386 process can be added to yield:



387 In the second type of sequential measurement process, the pointer-state QRF  $P$  is replaced  
 388 with an alternative QRF  $Q$  with which it does not commute. Sequences in which position  
 389 and momentum, or spins  $s_z$  and  $s_x$ , are measured alternately are examples. These can be  
 390 represented by the diagram:



391 As both  $P$  and  $Q$  must commute with  $R$ , the commutativity requirements for  $S$  are satisfied.  
 392 The sequences of operations depicted in Diagrams (6) and (7) clearly raise the questions  
 393 of how control is implemented, and of how the context changes that drive control flow are

394 detected. Before turning to these questions in Part II, we review a path-integral repre-  
 395 sentation of QRFs, show that the same representation also captures the behavior of any  
 396 system  $X$  identified by a QRF, and discuss the questions of multiple observers and quantum  
 397 contextuality.

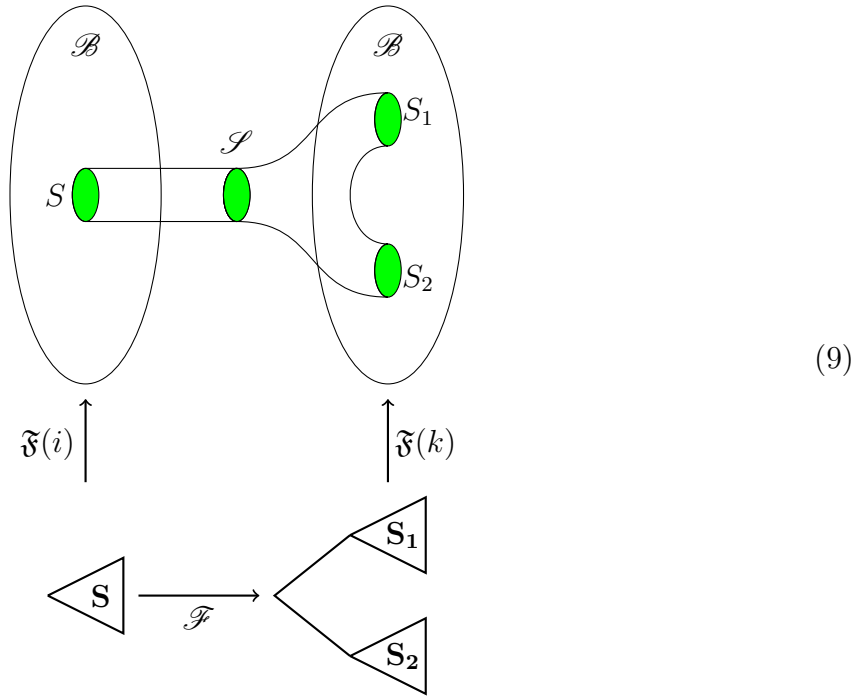
### 398 **2.3 The TQFT picture**

399 As a least-action principle, the FEP is fundamentally a statement about the paths followed  
 400 by the joint system  $U$  through its state space. The classical FEP is amenable to a path-  
 401 integral formulation [13] that expresses the expected value of any observable (functional)  
 402  $\Omega[x(t)]$  of paths  $x(t)$  through the relevant state space as ([101], Eq. 6):

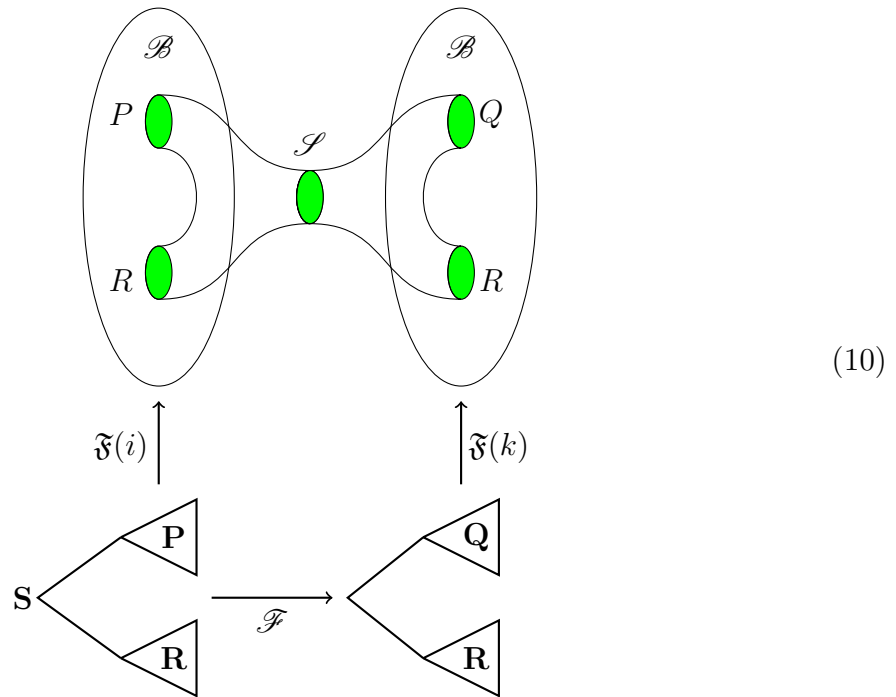
$$\langle \Omega[x(t)] \rangle = \int dx_0 \int d[x(t)] \Omega[x(t)] p(x(t)|x_0) p_0(x_0) \quad (8)$$

403 where  $x_0$  is the initial state and  $p(x(t)|x_0)$  is the conditional probability of the path  $x(t)$ .  
 404 Quantum theory generalizes this expression by, effectively, replacing  $\Omega[x(t)]$  with an au-  
 405 tomorphism on the relevant Hilbert space and  $p(x(t)|x_0)$  with an amplitude for  $x(t)$  given  
 406 the initial state  $x_0$ . For some finite-dimensional Hilbert space  $\mathcal{H}$ , the manifold of all such  
 407 automorphisms is a cobordism on  $\mathcal{H}$ , which is by definition a TQFT on  $\mathcal{H}$  [102].

408 We show in [59] that any sequential measurement of any sector  $X$  of  $\mathcal{B}$  induces a TQFT on  
 409  $X$ , considered as a projection of the  $N$ -dimensional boundary Hilbert space  $\mathcal{H}_{q_i}$  associated  
 410 with  $\mathcal{B}$ . In particular, measurement sequences of the form of Diagram (6) can be mapped  
 411 to cobordisms, i.e., to manifolds of maps between two designated boundaries, of the form:



412 while sequences of the form of Diagram (7) can be mapped to cobordisms of the form:



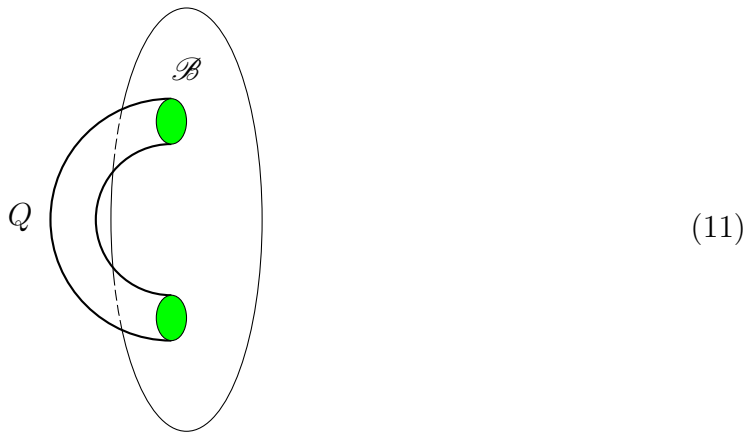
413 In either case,  $\mathfrak{F} : \mathbf{CCCD} \rightarrow \mathbf{Cob}$  is the functor from the category  $\mathbf{CCCD}$  of CCCDs (and

414 hence of QRFs) to the category **Cob** of finite cobordisms required to define a TQFT. In  
 415 general, we can state:

416 **Theorem 1** ([59] Thm. 1). *For any morphism  $\mathcal{F}$  of CCCDs in **CCCD**, there is a cobor-*  
 417 *dism  $\mathcal{S}$  such that a diagram of the form of Diagram (9) or (10) commutes.*

418 referring to [59] for the proof.

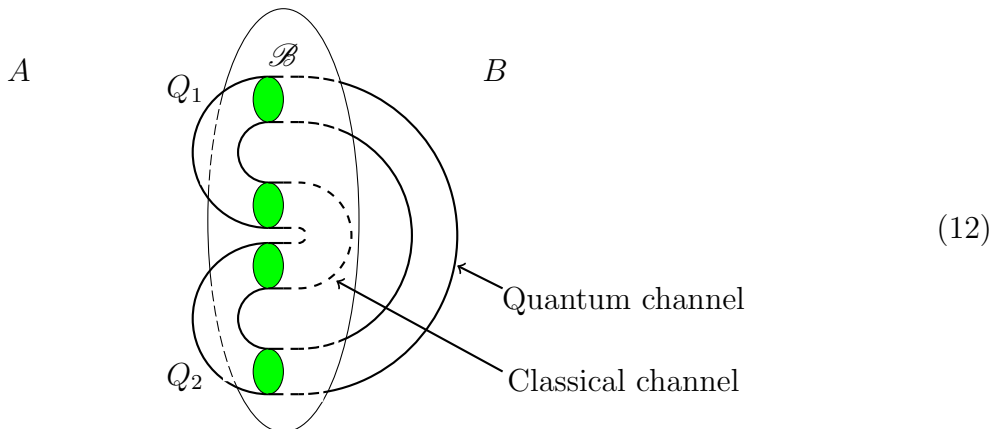
419 Theorem 1 applies to any sequential measurement; therefore, it applies to measurements  
 420 of a sector  $X$  followed by measurements of the associated memory sector  $Y$ , or vice versa.  
 421 Assuming for convenience that the dimension  $\dim(X) = \dim(Y)$ , we can consider a com-  
 422 posite operation  $Q = (\vec{Q}, \overleftarrow{Q})$ , where  $\vec{Q} = Q_X Q_Y$  and  $\overleftarrow{Q} = Q_Y Q_X$ . This  $Q$  is a pair of  
 423 QRF sequences that can be identified with TQFTs that measure and record an outcome,  
 424 mapping  $\mathcal{H}_X \rightarrow \mathcal{H}_Y$ , and dually use an outcome read from memory to prepare a state,  
 425 mapping  $\mathcal{H}_Y \rightarrow \mathcal{H}_X$ , respectively, as in Diagram 11:



426 This composite operator  $Q$  is, by Theorem 1, itself a TQFT [98]. Hence the operation of  
 427 recording observational outcomes for a sector  $X$  made at  $t$  to memory, and then comparing  
 428 them to later observations at  $t + \Delta t$ , is formally equivalent to propagating the “system”  $X$   
 429 forward in time from  $t$  to  $t + \Delta t$ .

430 Identifying QRFs as “internal” TQFTs allows a general analysis of information exchange

431 between multiple QRFs deployed by a single system, e.g.,  $A$ . Because all QRFs act on  
 432  $\mathcal{B}$ , information exchange between QRFs requires a channel that traverses  $B$ . Any such  
 433 channel is itself a QRF, one deployed by  $B$ . Considering  $A$  to comprise two observers,  
 434 one deploying  $Q_1$  and the other deploying  $Q_2$ , that interact via a local operations, classical  
 435 communication (LOCC [103]) protocol provides an example:



436 In a LOCC protocol, one channel is considered “classical” while the other is considered  
 437 “quantum”; however, this language masks the fact that both channels are physical. As  
 438 pointed out in [104], all media supporting classical communication are physical, and inter-  
 439 actions with these media are always local measurements or preparations. Hence the two  
 440 channels in a LOCC protocol are physically equivalent – both are TQFTs implemented by  
 441  $B$  – although their conventional semantics are different.

442 Diagram (12) can, clearly, also represent externally-mediated communication between any  
 443 two functional components of a system, e.g., macromolecular pathways within a cell or  
 444 functional networks within a brain. We show in [98] that whenever  $Q_1$  and  $Q_2$  are deployed  
 445 by distinct – technically, separable or mutually decoherent – “observers” or “systems,” they  
 446 fail to commute, i.e., the commutator  $[Q_1, Q_2] = Q_1Q_2 - Q_2Q_1 \geq h/2$ , where again  $h$  is  
 447 Planck’s constant. As shown in [57], Theorem 3.4 using the CCCD representation, non-  
 448 commutativity of QRFs induces quantum contextuality, i.e., dependence of measurement



449 results on “non-local hidden variables” that characterize the measurement context [105,  
450 106, 107]. In the current context, such hidden variables characterize the action of  $H_B$  on  
451  $\mathcal{B}$ , affecting what  $A$  will observe next in every cycle of  $A$ - $B$  interaction.

452 As shown in [63], such context dependence can, in principle, be captured classically if  
453 sufficient measurements of the context can be implemented. Such measurements would,  
454 however, have to access all of  $B$ . The existence of an MB prevents such access; in the  
455 current setting,  $A$  has access to  $B$  only via  $\mathcal{B}$ . The finite energetic cost of measurement,  
456 and consequent requirement for a thermodynamic sector  $F$ , prevents measurement even of  
457 all of  $\mathcal{B}$  by any finite physical system. Hence, we can expect physical systems, including  
458 all biological systems, to employ only local context-dependent control to switch between  
459 mutually non-commuting (sets of) QRFs. How context switches implemented by QRF  
460 switches induce evolution, development and learning was introduced in [22]. Some specific  
461 examples of context switching in biological systems will be discussed Part II.

### 462 **3 Conclusion**

463 We have shown in this Part I how the problem of defining control flow arises in active infer-  
464 ence systems, and provided three formal representations of the problem. Control flow can,  
465 in particular, be represented as switching between classical dynamical attractors, between  
466 deployed QRFs, and between computational processes represented by TQFTs. Implement-  
467 ing control flow has a free-energy cost; hence any control-flow system must trade off its own  
468 processing costs against the expected benefits of switching between input/output modes.  
469 The time and memory dependence of control flow can, moreover, be expected to lead  
470 generically to context effects on both perception and action.

471 In the accompanying Part II of this paper, we will first prove that control flows in active  
472 inference systems can always be represented as TNs, and show how TN architectures provide

473 a convenient classification control flows. We then show how these can be implemented by  
474 TQNNs, and discuss applications of this formalism to the problem of characterizing control  
475 flow in biological systems.

## 476 **Acknowledgements**

477 K.F. is supported by funding for the Wellcome Centre for Human Neuroimaging (Ref:  
478 205103/Z/16/Z), a Canada-UK Artificial Intelligence Initiative (Ref: ES/T01279X/1) and  
479 the European Union’s Horizon 2020 Framework Programme for Research and Innovation  
480 under the Specific Grant Agreement No. 945539 (Human Brain Project SGA3). M.L. grate-  
481 fully acknowledges funding from the Guy Foundation and the John Templeton Foundation,  
482 Grant 62230. A.M. wishes to acknowledge support by the Shanghai Municipality, through  
483 the grant No. KBH1512299, by Fudan University, through the grant No. JJH1512105,  
484 the Natural Science Foundation of China, through the grant No. 11875113, and by the  
485 Department of Physics at Fudan University, through the grant No. IDH1512092/001.

## 486 **Conflict of interest**

487 The authors declare no competing, financial, or commercial interests in this research.

## 488 **References**

- 489 [1] Friston KJ. A theory of cortical responses. *Philos Trans R Soc Lond B, Biol Sci*  
490 2005;360:815–36.
- 491 [2] Friston KJ, Kilner J, Harrison L. A free energy principle for the brain. *J Physiol Paris*  
492 2006;100:70–87.

- 493 [3] Friston KJ, Stephan KE. Free-energy and the brain. *Synthese* 2007;159:417–58.
- 494 [4] Friston, K. J. 2010 The free-energy principle: A unified brain theory? *Nature Reviews*  
495 *Neuroscience* 11, 127–138.
- 496 [5] Friston, K. J. 2013 Life as we know it. *Journal of The Royal Society Interface* 10,  
497 20130475.
- 498 [6] Friston KJ, FitzGerald T, Rigoli F, Schwartenbeck P, Pezzulo G. Active inference: a  
499 process theory. *Neural Comput* 2017;29:1–49.
- 500 [7] Ramstead MJ, Badcock PB, Friston KJ. Answering Schrödinger’s question: a free-  
501 energy formulation. *Phys Life Rev* 2018;24:1–16.
- 502 [8] Ramstead MJ, Constant A, Badcock PB, Friston KJ. 2019 Variational ecology and  
503 the physics of sentient systems. *Phys Life Rev* 31, 188–205.
- 504 [9] Kuchling F, Friston K, Georgiev G, Levin M. 2020 Morphogenesis as Bayesian infer-  
505 ence: A variational approach to pattern formation and control in complex biological  
506 systems. *Phys Life Rev* 33, 88–108.
- 507 [10] Friston, K. J. 2019 A free energy principle for a particular physics. Preprint  
508 arxiv:1906.10184 [q-bio.NC]. <https://arxiv.org/abs/1906.10184>
- 509 [11] Ramstead MJ, Sakthivadivel DAR, Heins C, Koudahl M, Millidge B, Da Costa L,  
510 Klein B, Friston KJ 2022 On Bayesian mechanics: A physics of and by beliefs. *Inter-*  
511 *face Focus* 13, 2022.0029.
- 512 [12] Fields C, Friston K, Glazebrook JF, Levin M 2022 A free energy principle for generic  
513 quantum systems. *Prog. Biophys. Mol. Biol.* 173, 36–59.

- 514 [13] Friston, K., Da Costa, L., Sakthivadivel, D. A. R., Heins, C., Pavliotis, G. A., Ram-  
515 stead, M., Parr, T. 2022 Path integrals, particular kinds, and strange things. Preprint  
516 arxiv:2210.12761.
- 517 [14] Pearl, J. 1988 *Probabilistic Reasoning in Intelligent Systems: Networks of Plausible*  
518 *Inference*. San Mateo CA: Morgan Kaufmann.
- 519 [15] Clark A. 2017 How to knit your own Markov blanket: Resisting the second law with  
520 metamorphic minds. In (T. Wetzinger and W. Wiese, eds.) *Philosophy and Predictive*  
521 *Processing 3*, 19pp. Frankfurt am Main: Mind Group.
- 522 [16] Kirchhoff, M., Parr, T., Palacios, E., Friston, K., Kiverstein, J. 2018 The Markov  
523 blankets of life: Autonomy, active inference and the free energy principle. *J. R. Soc.*  
524 *Interface* 15, 20170792.
- 525 [17] Parr, T., Da Costa, L., Friston, K. 2020 Markov blankets, information geometry and  
526 stochastic thermodynamics. *Philos. Trans. A: Math. Phys. Eng. Sci.* 378, 20190159.
- 527 [18] Sakthivadivel, D.A.R. 2022 Weak Markov blankets in high-dimensional, sparsely-  
528 coupled random dynamical systems. Preprint arXiv:2207.07620.
- 529 [19] Wheeler, J. H. 1989 Information, physics, quantum: The search for links. In: Zurek,  
530 W. (Ed.), *Complexity, Entropy, and the Physics of Information*. CRC Press, Boca  
531 Raton, FL, pp. 3–28.
- 532 [20] Levin, M. 2019 The computational boundary of a “self”: Developmental bioelectricity  
533 drives multicellularity and scale-free cognition. *Front. Psychol.* 10, 1688.
- 534 [21] Levin, M. 2021 Life, death, and self: Fundamental questions of primitive cognition  
535 viewed through the lens of body plasticity and synthetic organisms. *Biochem. Biophys.*  
536 *Res. Commun.* 564, 114–133.

- 537 [22] Fields, C.; Glazebrook, J. F.; Levin, M. 2021 Minimal physicalism as a scale-free  
538 substrate for cognition and consciousness. *Neurosci. Cons.* 7(2), niab013.
- 539 [23] Levin, M. 2022 Technological approach to mind everywhere: An experimentally-  
540 grounded framework for understanding diverse bodies and minds. *Front. Syst. Neu-*  
541 *rosci.* 16, 768201.
- 542 [24] Endsley, M. R. 2012 Situational awareness. In: Salvendy, G. (Ed.) *Handbook of Hu-*  
543 *man Factors and Ergonomics*, 4th Ed. Hoboken, NJ, John Wiley, pp. 553–568.
- 544 [25] Fields, C.; Levin, M. 2018 Multiscale memory and bioelectric error correction in the  
545 cytoplasm-cytoskeleton-membrane system. *WIREs Syst. Biol. Med.* 10, e1410.
- 546 [26] Clark, A., Chalmers, D. 1998 The extended mind (Active externalism). *Analysis*  
547 58(1), 7–19.
- 548 [27] Anderson, M. L. 2003 Embodied cognition: A field guide. *Artif. Intell.* 149, 91–130.
- 549 [28] Froese, T., Ziemke, T 2009 Enactive artificial intelligence: Investigating the systemic  
550 organization of life and mind. *Artif. Intell.* 173, 466–500.
- 551 [29] Attias, H. 2003 Planning by probabilistic inference. *Proc. of the 9th Int. Workshop*  
552 *on Artificial Intelligence and Statistics* in Proc. Machine Learning Res. R4, 9–16.
- 553 [30] Botvinick, M., Toussaint, M. 2012 Planning as inference. *Trends Cogn. Sci.* 16(10),  
554 485–488.
- 555 [31] Lanillos, P., Mio, C., Pezzato, C., et al. 2021 Active inference in robotics and artificial  
556 agents: Survey and challenges. Preprint arXiv:2112.01871.
- 557 [32] Chubukov, V., Gerosa, L., Kochanowski, K., Sauer, U. 2014 Coordination of microbial  
558 metabolism. *Nat. Rev. Microbiol.* 12, 327–340.

- 559 [33] Micali, G., Endres, R. G. 2016 Bacterial chemotaxis: information processing, ther-  
560 modynamics, and behavior. *Curr. Opin. Microbiol.* 30, 8–15.
- 561 [34] Pezzulo, G., LaPalme, J., Durant, F., Levin, M. 2021 Bistability of somatic pattern  
562 memories: stochastic outcomes in bioelectric circuits underlying regeneration. *Philos.*  
563 *Trans. R. Soc. Lond. B* 376(1821), 20190765.
- 564 [35] Blake, R., Logothetis, N. K. 2002 Visual competition. *Nat. Rev. Neurosci.* 3, 1–11.
- 565 [36] Stertzer, P., Kleinschmidt, A., Rees, G. 2009 The neural bases of multistable percep-  
566 tion. *Trends Cogn. Sci.* 13, 310–318.
- 567 [37] Schwartz, J.-L., Grimault, N., Hupé, J.-M., Moore, B. C. J., Pressnitzer, D. 2012  
568 Multistability in perception: bindingsensory modalities, An overview. *Phil. Trans. R.*  
569 *Soc. Lond. B* 367, 896–905.
- 570 [38] Vossel, S., Geng, J. J., Fink, G. R. 2014 Dorsal and ventral attention systems: Distinct  
571 neural circuits but collaborative roles. *Neuroscientist* 20, 150–159.
- 572 [39] Baars, B. J., Franklin, S. 2003 How conscious experience and working memory inter-  
573 act. *Trends Cogn. Sci.* 7, 166–172.
- 574 [40] Baars, B. J., Franklin, S., Ramsøy, T. Z. 2013 Global workspace dynamics: Cortical  
575 “binding and propagation” enables conscious contents. *Front. Psychol.* 4, 200.
- 576 [41] Kuchling, F.; Fields, C.; Levin, M. 2022 Metacognition as a consequence of competing  
577 evolutionary time scales. *Entropy* 24, 601.
- 578 [42] Parr, T., Friston, K. J. 2019 Generalised free energy and active inference. *Biol. Cy-*  
579 *bern.* 113(5-6), 495–513.
- 580 [43] Winn, J. Bishop, C. M. 2005 Variational message passing. *J. Mach. Learn. Res.* 6,  
581 661–694.

- 582 [44] Dauwels, J. 2007 On variational message passing on factor graphs. *2007 IEEE Inter-*  
583 *national Symposium on Information Theory*, Nice, France.
- 584 [45] Parr, T., Sajid, N., Friston, K. J. 2020 Modules or mean-fields? *Entropy* 22(5), 552.
- 585 [46] Da Costa, L., Parr, T. Sajid, N., Veselic, S., Neacsu, V., Friston, K. 2020 Active  
586 inference on discrete state-spaces: A synthesis. *J. Math. Psychol.* 99, 102447.
- 587 [47] Friston, K., Parr, T., de Vries, B. 2017 The graphical brain: Belief propagation and  
588 active inference. *Netw. Neurosci.* 1(4), 381–414.
- 589 [48] Orús, R. 2019 Tensor networks for complex quantum systems. *Nat. Rev. Phys.* 1,  
590 538–550.
- 591 [49] Bao, N., Cao, C.-J., Carroll, S. M., Chatwin-Davies, A. 2017 de Sitter space as a  
592 tensor network: Cosmic no-hair, complementarity, and complexity. *Phys. Rev. D* 96,  
593 123536.
- 594 [50] Hu, Q., Vidal, G. 2017 Spacetime symmetries and conformal data in the continuous  
595 Multiscale Entanglement Renormalization Ansatz. *Phys. Rev. Lett.* 119, 010603.
- 596 [51] Chandra, A. R., de Boer, J., Flory, M., Heller, M. P., Hörtner, S., Rolph, A. 2021  
597 Spacetime as a quantum circuit. *J. High Energy Phys.* 2021, 207.
- 598 [52] Aharonov Y, Kaufherr T. Quantum frames of reference. *Phys Rev D* 1984;30:368–385.
- 599 [53] Bartlett SD, Rudolph T, Spekkens RW. 2007 Reference frames, super-selection rules,  
600 and quantum information. *Rev Mod Phys* 79, 555–609.
- 601 [54] Barwise, J.; Seligman, J. 1997 *Information Flow: The Logic of Distributed Systems*  
602 (Cambridge Tracts in Theoretical Computer Science 44). Cambridge University Press,  
603 Cambridge, UK.

- 604 [55] Fields, C.; Glazebrook, J. F. 2019 A mosaic of Chu spaces and Channel Theory I:  
605 Category-theoretic concepts and tools. *J. Expt. Theor. Artif. intell.* 31, 177–213.
- 606 [56] Fields, C.; Glazebrook, J. F. 2020 Representing measurement as a thermodynamic  
607 symmetry breaking. *Symmetry* 12, 810.
- 608 [57] Fields, C.; Glazebrook, J. F. 2022 Information flow in context-dependent hierarchical  
609 Bayesian inference. *J. Expt. Theor. Artif. intell.* 34, 111–142.
- 610 [58] Fields, C.; Glazebrook, J. F.; Marcianò, A. 2021 Reference frame induced symmetry  
611 breaking on holographic screens. *Symmetry* 13, 408.
- 612 [59] Fields, C.; Glazebrook, J. F.; Marcianò, A. (2022) Sequential measurements, topo-  
613 logical quantum field theories, and topological quantum neural networks. *Fortschr.*  
614 *Phys.* 2022, 2200104.
- 615 [60] Abramsky, S., Brandenburger, A. 2011 The sheaf-theoretic structure of non-locality  
616 and contextuality. *New J. Phys.* 13, 113036.
- 617 [61] Abramsky, S., Barbosa, R. S., Mansfield, S. 2017 Contextual fraction as a measure  
618 of contextuality. *Phys. Rev. Lett.* 119, 050504.
- 619 [62] Dzhafarov, E. N.; Kujala, J. V. (2017a). Contextuality-by-Default 2.0: Systems with  
620 binary random variables. In: J. A. Barros, B. Coecke and E. Pothos (eds.) *Lecture*  
621 *Notes in Computer Science* 10106, Springer, Berlin, 16–32.
- 622 [63] Dzhafarov, E. N. & Kon, M. 2018 On universality of classical probability with con-  
623 textually labeled random variables. *J. Math. Psychol.* 85, 17–24.
- 624 [64] Adlam, E. 2021 Contextuality, fine-tuning and teleological explanation. *Found. Phys.*  
625 51, 106.



- 626 [65] Marcianò, A.; Chen, D.; Fabrocini, F.; Fields, C.; Greco, E.; Gresnigt, N.; Jinklub,  
627 K.; Lulli, M., Terzidis, K.; Zappala, E. 2022 Quantum neural networks and topological  
628 quantum field theories. *Neural Networks* 153, 164–178.
- 629 [66] Marcianò, A., Chen, D., Fabrocini, F., Fields, C., Lulli, M., Zappala, E. 2022 Deep  
630 neural networks as the semi-classical Limit of topological quantum neural networks:  
631 The problem of generalisation. Preprint arXiv:2210.13741.
- 632 [67] Sterling, P., Eyer, J. 1988 Allostasis: A new paradigm to explain arousal pathology.  
633 In: *Handbook of Life Stress, Cognition and Health*. John Wiley & Sons: New York,  
634 pp. 629–649.
- 635 [68] Barrett, L. F., Quigley, K. S., Hamilton, P. 2016 An active inference theory of al-  
636 lostasis and interoception in depression. *Philos. Trans. R. Soc. Lond. B Biol. Sci.*  
637 371(1708), 20160011.
- 638 [69] Corcoran, A. W., Pezzulo, G., Hohwy, J. 2020 From allostatic agents to counterfactual  
639 cognisers: Active inference, biological regulation, and the origins of cognition. *Biol.*  
640 *Philos.* 35(3), 32.
- 641 [70] Hohwy, J. 2016 The self-evidencing brain. *Nou̇s* 50(2), 259–285.
- 642 [71] Sakthivadivel, D. A. R. 2022 A constraint geometry for inference and integration.  
643 Preprint arXiv:2203.08119.
- 644 [72] Sakthivadivel, D. A. R. 2022 Towards a geometry and analysis for Bayesian mechanics.  
645 Preprint arXiv:2204.11900.
- 646 [73] Landauer, R. 1961 Irreversibility and heat generation in the computing process. *IBM*  
647 *J. Res. Dev.* 5, 183–195.

- 648 [74] Jarzynski, C. 1997 Nonequilibrium equality for free energy differences. *Phys. Rev.*  
649 *Lett.* 78(14), 2690–2693.
- 650 [75] Evans, D. J. 2003 A non-equilibrium free energy theorem for deterministic systems.  
651 *Molec. Phys* 101(10), 1551–1554.
- 652 [76] Friston, K., Thornton, C., Clark, A. 2012 Free-energy minimization and the dark-  
653 room problem. *Front. Psychol.* 3, 130.
- 654 [77] Pezzulo, G., Rigoli, F., Friston, K. 2015 Active Inference, homeostatic regulation and  
655 adaptive behavioural control. *Prog. Neurobiol.* 134, 17–35.
- 656 [78] Friston, K., Rigole, F., Ognibene, D., Mathys, C., Fitzgerald, T., Pezzulo, G. 2015  
657 Active inference and epistemic value. *Cogn. Neurosci.* 6, 187-214.
- 658 [79] Schmidhuber, J. 1991 Curious model-building control-systems. *1991 IEEE Interna-*  
659 *tional Joint Conference on Neural Networks*, Vols 1-3; 2, 1458–1463.
- 660 [80] Sun, Y., Gomez, F., Schmidhuber, J. 2011 Planning to be surprised: Optimal  
661 Bayesian exploration in dynamic environments. *Artificial General Intelligence*. J.  
662 Schmidhuber, K. R. Thórisson and M. Looks, Eds. Berlin, Heidelberg, Springer. pp.  
663 41–51.
- 664 [81] Sengupta, B., Friston, K. 2018 How Robust are deep neural networks? Preprint arXiv  
665 arXiv:1804.11313.
- 666 [82] Seth, A. K., Friston, K. J. 2016 Active interoceptive inference and the emotional  
667 brain. *Philos. Trans. R. Soc. Lond. B* 371(1708), 20160007.
- 668 [83] Emmons-Bell, M., Durant, F., Hammelman, J. et al. 2015 Gap junctional blockade  
669 stochastically induces different species-specific head anatomies in genetically wild-  
670 type *Girardia dorotocephala* flatworms. *Int. J. Mol. Sci.* 16, 27865–27896.

- 671 [84] Oviedo, N. J., J. Morokuma, Walentek, P. et al. 2010 Long-range neural and gap  
672 junction protein-mediated cues control polarity during planarian regeneration. *Dev.*  
673 *Biol.* 339, 188–199.
- 674 [85] Tegmark M 2000 Importance of quantum decoherence in brain processes. *Phys. Rev.*  
675 *E* 61: 4194–4206.
- 676 [86] Schlosshauer M. 2007 *Decohenece and the Quantum to Classical Transition*. Springer,  
677 Berlin.
- 678 [87] Zweir MC, Chong LT. 2010 Reaching biological timescales with all-atom molecular  
679 dynamics simulations. *Curr. Opin. Pharmacol.* 10: 745–752.
- 680 [88] Marais A *et al.* 2018 The future of quantum biology. *J. R. Soc. Interface* 15: 20180640.
- 681 [89] Cao J *et al.* 2020 Quantum biology revisited. *Science Adv.* 6: eaaz4888.
- 682 [90] Kim, Y., Bertagna, F., D’Souza, E. M., Heyes, D. J., Johannissen, L. O., Nery, E. T.  
683 2021 Quantum biology: an update and perspective. *Quant. Rep.* 3, 1–48.
- 684 [91] Baiardi, A., Christandl, M., Reiher, M. 2022 Quantum computing for molecular bi-  
685 ology. Preprint arxiv:2212.12220.
- 686 [92] Fields, C.; Levin, M. 2021 Metabolic limits on classical information processing by  
687 biological cells. *BioSystems* 209, 104513.
- 688 [93] Kerskens, C. M., Pérez, D. L. 2022 Experimental indications of non-classical brain  
689 functions. *J. Phys. Commun.* 6, 105001.
- 690 [94] Fields, C.; Marcianò, A. 2019 Holographic screens are classical information channels.  
691 *Quant. Rep.* 2, 326–336.

- 692 [95] Addazi, A.; Chen, P.; Fabrocini, F.; Fields, C.; Greco, E.; Lulli, M.; Marcianò,  
693 A.; Pasechnik, R. 2021 Generalized holographic principle, gauge invariance and the  
694 emergence of gravity à la Wilczek. *Front. Astron. Space Sci.* 8, 563450.
- 695 [96] Fields, C.; Glazebrook, J. F.; Marcianò, A. 2022 The physical meaning of the holo-  
696 graphic principle. *Quanta* 11, 72–96.
- 697 [97] Pastawski, F.; Yoshida, B.; Harlow, D.; Preskill, J. 2015 Holographic quantum error-  
698 correcting codes: Toy models for the bulk/boundary correspondence. *J. High Energy*  
699 *Phys.* 6, 149.
- 700 [98] Fields, C.; Glazebrook, J. F.; Marcianò, A. 2023 Communication protocols and quan-  
701 tum error-correcting codes from the perspective of topological quantum field theory.  
702 Preprint arxiv:2303.16461 [hep-th].
- 703 [99] Landauer, R. 1999 Information is a physical entity. *Physica A* 263, 63–67.
- 704 [100] Bennett, C. H. 1982 The thermodynamics of computation. *Int. J. Theor. Phys.* 21,  
705 905–940.
- 706 [101] Seifert, U. 2012 Stochastic thermodynamics, fluctuation theorems and molecular ma-  
707 chines. *Rep. Prog. Phys.* 75, 126001.
- 708 [102] Atiyah, M. 1988 Topological quantum field theory. *Pub. Math. IHÉS* 68, 175–186.
- 709 [103] Chitambar, E., Leung, D., Mančinska, L., Ozols, M., Winter, A. 2014 Everything you  
710 always wanted to know about LOCC (but were afraid to ask). *Comms. Math. Phys.*  
711 328, 303–326.
- 712 [104] Tipler, F. 2014 Quantum nonlocality does not exist. *Proc. Natl. Acad. Sci. USA* 111,  
713 11281–11286.

- 714 [105] Bell, J. S. 1966 On the problem of hidden variables in quantum mechanics. *Rev. Mod.*  
715 *Phys.* 38, 447–452.
- 716 [106] Kochen, S., Specker, E. P. 1967 The problem of hidden variables in quantum mechan-  
717 ics. *J. Math. Mech.* 17, 59–87.
- 718 [107] Mermin, N. D. 1993 Hidden variables and the two theorems of John Bell. *Rev. Mod.*  
719 *Phys.* 65, 803–815.